© 2014. Published by The Company of Biologists Ltd | The Journal of Experimental Biology (2014) 217, 2590-2600 doi:10.1242/jeb.105429

RESEARCH ARTICLE

Jumping mechanisms in flatid planthoppers (Hemiptera, Flatidae)

Malcolm Burrows*

ABSTRACT

The jumping performance of three species of hemipterans from Australia and Europe belonging to the family Flatidae was analysed from images captured at a rate of 5000 s^{-1}. The shape of a flatid was dominated by large triangular or wedge-shaped front wings, which, when folded, covered and extended above and behind the body to give a laterally compressed and possibly streamlined appearance. The body lengths of the three species of adults ranged from 7 to 9 mm and their mass from 8 to 19 mg. The propulsive hind legs were 30% longer than the front legs but only 36–54% of the body length. Jumps with the fastest take-off velocities of 2.8–3.2 m s^{-1} had acceleration times of 1.4–1.8 ms. During such jumps, adults experienced an acceleration of 174–200 ***g***. These jumps required an energy expenditure of 76–225 µJ, a power output of 13–60 mW and exerted a force of 9–37 mN. The required power output per mass of jumping muscle in adults ranged from 24,000 to 27,000 W kg^{-1} muscle, 100 times greater than the maximum active contractile limit of normal muscle. The free-living nymphs were also proficient jumpers, reaching take-off velocities of 2.2 m s^{-1}. To achieve such a jumping performance requires a power amplification mechanism. The energy store for such a mechanism was identified as the internal skeleton linking a hind coxa to the articulation of a hind wing. These pleural arches fluoresced bright blue when illuminated with UV light, indicating the presence of the elastic protein resilin. The energy generated by the prolonged contractions of the trochanteral depressor muscles was stored in distortions of these structures, and the rapid elastic recoil of these muscles powered the synchronous propulsive movements of the hind legs.

KEY WORDS: Biomechanics, Kinematics, Energy storage, Resilin, Auchenorrhyncha

INTRODUCTION

The Hemiptera contains some of fastest and most powerful jumpers amongst all insects. The champion jumpers, as defined by their take-off velocities, belong to the sub-order Auchenorrhyncha, which contains three groups currently considered to be monophyletic (Cryan and Urban, 2012): the Cercopoidea (froghoppers), the Membracoidea (leafhoppers and treehoppers) and the Fulgoroidea (planthoppers). To produce their rapid and powerful jumps, all use a catapult-like mechanism in which rapid movements of the hind legs are powered by a pair of large muscles located in the thorax. These muscles have anatomical features of slow muscle (Burrows et al., 2014), even though in other insects they are part of the flight machinery and thus contract rapidly. The slow contractions of these muscles take place in advance of a jump and result in distortion and bending of bow-shaped parts of the internal skeleton that contain the elastic protein resilin (Burrows et al., 2008). Energy is stored slowly in these structures, allowing power to be amplified, and is then released suddenly as they unfurl and return to their original shape (Burrows, 2006; Burrows, 2007b; Burrows, 2009). To propel the body forwards, and without losing energy to spin, requires that hind legs both move at the same time. To produce such synchrony of action, froghoppers and planthoppers activate muscles of the left and right hind legs with a tightly coupled sequence of motor spikes, thereby ensuring that similar levels of force are developed by both in their primed, pre-jump position (Burrows, 2007c; Burrows and Bräunig, 2010). The neural control alone cannot, however, deliver the close synchrony that is needed. Adult planthoppers therefore use a mechanical mechanism in which a protrusion of one hind leg contacts a similar protrusion on the other hind leg (Burrows, 2010). The first hind leg to move thus nudges the other hind leg from its primed position. Nymphal planthoppers have a series of different protrusions on each hind leg (Heilig and Sander, 1986; Sander, 1957), which intermesh with each other and act like cog wheels (Burrows and Sutton, 2013). Again, the first hind leg to move will ensure that the other also moves at the same time. Both mechanisms ensure that the power generated by the hind legs is delivered within 0.03 ms of each other.

The planthopper group contains some 20 families that have a great diversity of body shapes. Jumping mechanisms and performance have been analysed in only two of these families, the Issidae and Dictyopharidae (Burrows, 2009; Burrows, 2014). Issids have a solid body with a squared-off front to the head, whereas dictyopharids are more delicate and have a pointed head that gives a streamlined appearance. The Flatidae, the subject of this paper, have a distinctively different body shape dominated by large, stiff front wings. When folded, these wings cover the body and most of the legs to give a laterally compressed and smooth appearance. This paper analyses the jumping mechanisms in three species of this family with the aim of determining how the different body shape might influence jumping performance. The jumping of the wingless nymphs is also analysed.

RESULTS

Body shape

The three species of flatid analysed here had triangular front wings that were held close to the body in a vertical position and so exaggerated and dominated their laterally compressed appearance when viewed from the side (Fig. 1). The wings projected well beyond the tip of the abdomen and in *Colgar peracutum* (Walker 1858) and *Siphanta acuta* (Walker 1851) almost touched the ground so that only the pointed head and the distal segments of the front and middle legs and sometimes the tarsus of the hind legs were visible (Fig. 1A,B). In adult *Metcalfa pruinosa* (Say 1830), the head was flattened anteriorly, and the wings were rounded dorsally and posteriorly to give a more wedge-shaped appearance to the whole insect in side view (Fig. 1C). The nymphs of *M. pruinosa* had many fine strands of wax covering the wingless body and protruding from the rear of the abdomen (Fig. 1D). The adult body lengths ranged from 7.4±0.1 mm in *C. peracutum* (mean ± s.e.m., *N*=29) to 7.9±0.2

Department of Zoology, University of Cambridge, Cambridge CB2 3EJ, UK.

*Author for correspondence (mb135@hermes.cam.ac.uk)

Received 14 March 2014; Accepted 23 April 2014

The Journal of Experimental Biology

The Journal of Experimental Biology (2014) doi:10.1242/jeb.105429

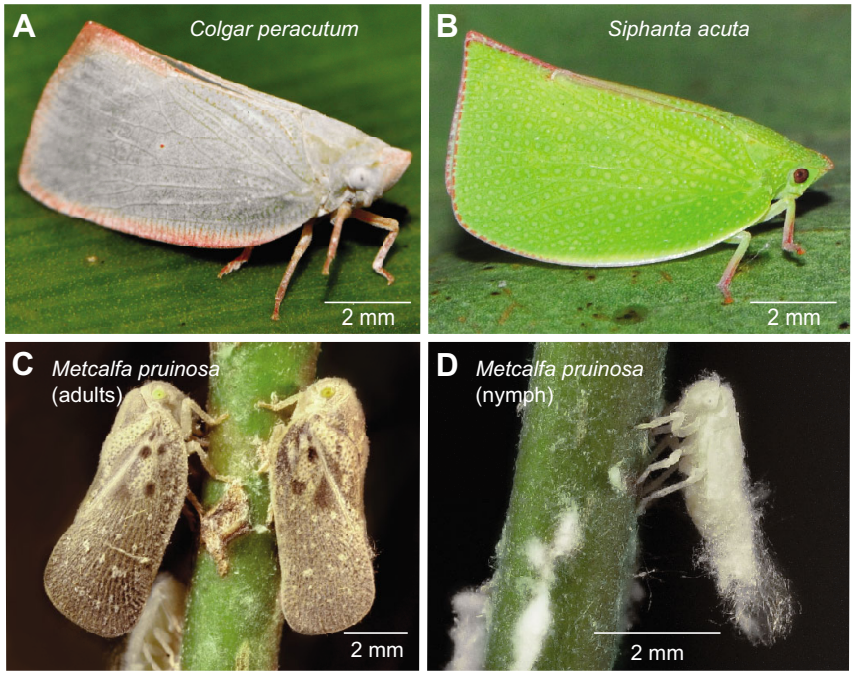

Fig. 1. Body form of the three species of flatid analysed in this paper. (A) Photograph of an adult *C. peracutum*. (B) An adult *S. acuta*. (C) An adult *M. pruinosa*. (D) A nymph of *M. pruinosa*. All photographs are side views.

in *M. pruinosa* (*N*=7) and 9.3 mm in *S. acuta* (Table 1). Some unidentified species found in Borneo, the jumping performance of which could not be studied, had body lengths of 15 mm and wings that were 30 mm long, giving a wingspan of ~50 mm. Body masses ranged from 8.3±0.9 mg in *M. pruinosa* to 19.3±1.3 mg in *C. peracutum* (Table 1). All had hind legs that were 30% longer than the front or middle legs so that the ratio of leg lengths was 1:1:1.3 (front:middle:hind) and none exceeded 54% of the body length, or gave a ratio greater than 1.6 relative to the cube root of body mass (Table 1). The increased length of a hind leg was due to its tibia, which was 43% longer than a middle tibia (Fig. 2A). The hind legs of *M. pruinosa* nymphs were 40% longer than the front and middle legs and were 81% of the body length (Table 1).

Structure of hind legs

The coxae of the hind legs were larger than those of the other legs and abutted against each other at the ventral midline of the body and extended to the lateral edges of the metathorax (Fig. 2B). The ventral surface of hind coxae was covered by a flexible, transparent membrane through which the tendon and part of the large trochanteral depressor muscle was visible. By contrast, the coxae of the front and middle legs were separated from each other at the midline so that the sheath of the piercing mouthparts could lie between them. They were also capable of greater rotation with their respective thoracic segments. Each small, cylindrical hind trochanter rotated through ~100 deg about a double pivot joint with its coxa, thus enabling both hind legs to be levated forwards and depressed backwards in the same plane almost parallel to the ventral surface of the body (Fig. 2C,D). The femur rotated a little about the trochanter, and the tibia rotated by more than 100 deg about the femur. The tibia was the longest segment of the leg and bore a single, stout spine and a group of smaller, ventrally pointing spines at the articulation of the tarsus (Fig. 2A). The first segment of the tarsus also had a series of spines at its articulation with the second segment and a pair of claws on the terminal segment (Fig. 2A). These small spines and the claws made contact with the ground and should improve traction when the hind legs propel a jump.

At the midline apposition of the two coxae, the inner surface of each had an array of small protrusions called microtrichia (Gorb, 2001), which interdigitated with those on the other coxa (Fig. 3A,B). The microtrichia increase the area of the opposed surfaces and should therefore strengthen resistance to movement between the two coxae. Both coxae thus provide a stable base from which movements of the more distal segments of the hind legs are made. Further microtrichia covered the entire surface of a large protrusion of the lateral and posterior wall of each coxa (Fig. 3C,D). These microtrichia were ~5 μm wide and 5 μm high and were spaced quite regularly at 5–6 μm intervals from the next one. At the base of the protrusion, each had a flattened rounded shape, which progressively became more pointed towards the tip of the protrusion. When the

Table 1. Body form of flatids

	Body mass (mg)	Body length (mm)	Hind leg, femur (mm)	Hind leg, tibia (mm)	Ratio of leg lengths			Hind leg length	
					Front	Middle	Hind	Percentage of body length	Length (mm)/ body mass$^{1/3}$ (mg)
C. peracutum (*N*=29)	19.3±1.3	7.4±0.1	1.0±0.05	1.8±0.06	1	1	1.3	54	1.4
S. acuta (*N*=3)	13.7	9.3	1.1	1.5	1	1	1.3	36	1.3
M. pruinosa, adults (*N*=7)	8.3±0.9	7.9±0.2	1.0±0.03	1.6±0.1	1	1.1	1.3	41	1.6
M. pruinosa, nymphs (*N*=7)	2.9±0.3	3.6±0.1	0.9±0.02	1.3±0.04	1	1.1	1.4	81	2.0

Body length and mass, and the lengths of the hind femora and tibiae in the three species of flatid analysed; *N* indicates the number of individuals from which the measurements were taken. The ratio of leg lengths is given relative to the front legs.

The Journal of Experimental Biology (2014) doi:10.1242/jeb.105429

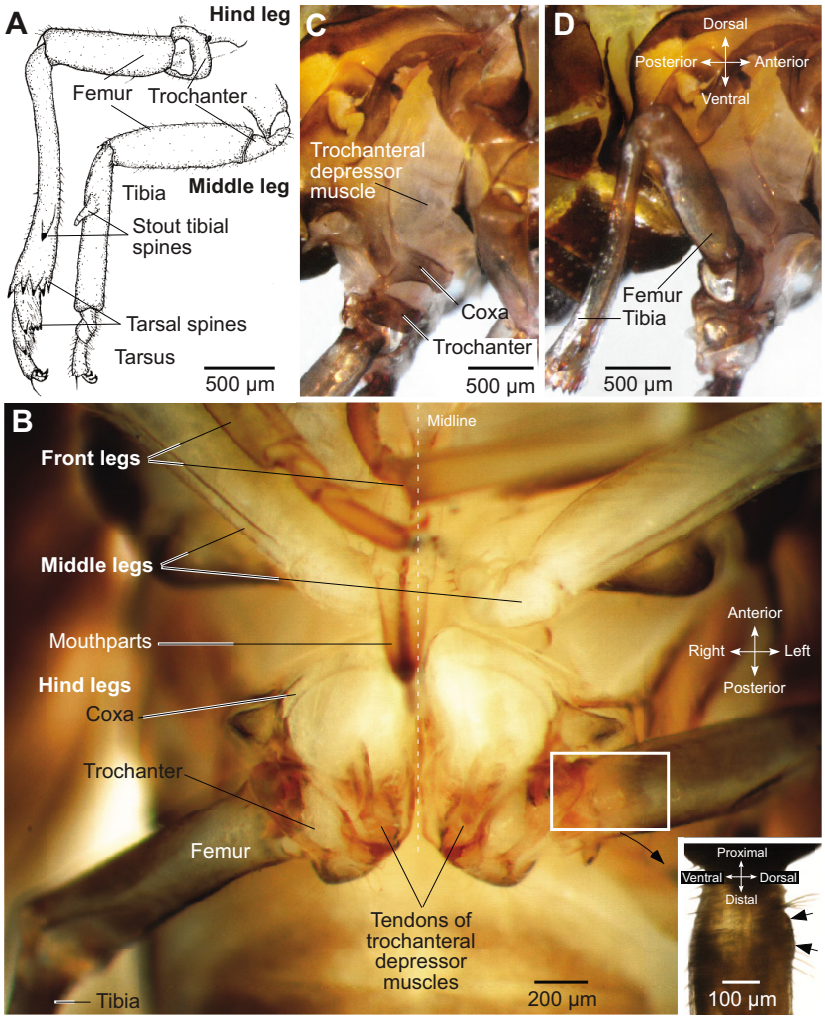

Fig. 2. Hind legs of *C. peracutum*. (A) Drawings of the right hind and right middle leg. (B) Ventral view of the proximal joints of the hind legs. Both trochantera are partially levated about their respective coxae. The sheath of the piercing mouthparts projects between the coxae of the middles legs and ventral to the hind coxae. The white box and inset show an enlarged view of the dorsal femur of the hind leg. A flat raised region (black arrows) has tufts of long hairs on its proximal and distal borders. (C) Lateral view of the right side of the thorax with the right hind leg depressed at the coxo-trochanteral joint. The lateral cuticle of the metathorax has been removed to reveal the large trochanteral depressor muscle of the right hind leg. (D) Lateral view with the right hind leg fully levated at its coxo-trochanteral joint and the depressor muscle is still visible.

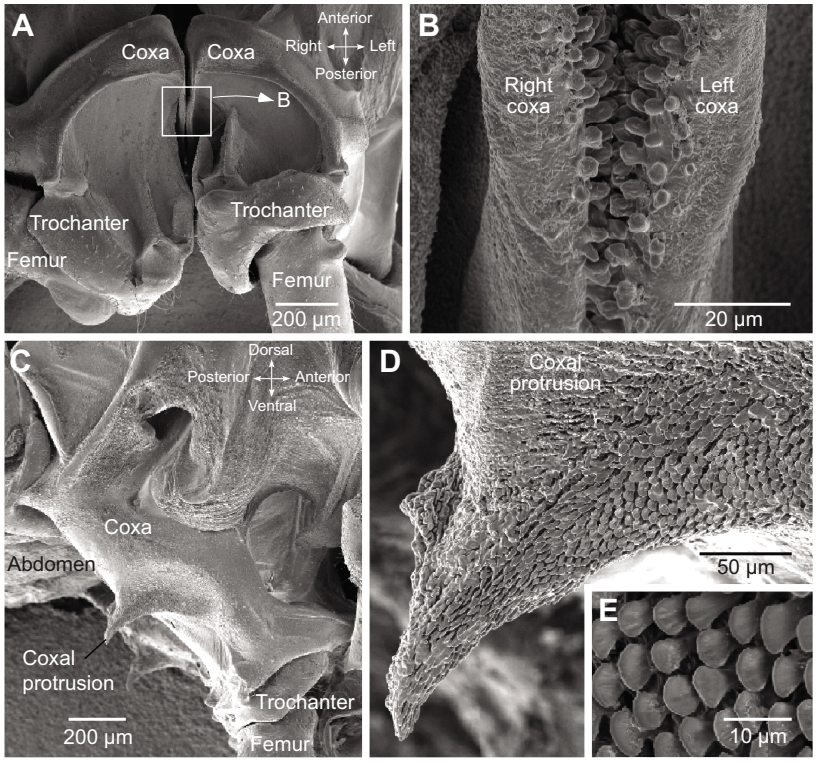

Fig. 3. Scanning electron micrographs of the hind legs of *C. peracutum*. (A) Ventral view of the coxo-trochanteral and trochantero-femoral joints. The trochanter on the left is levated about its coxa, and on the right is depressed. (B) Enlarged view of the region demarcated by the box in A to show that the close apposition of the two coxae medially is enhanced by the interlocking of small protrusions from each. (C) Lateral view of the right metathorax with the trochanter fully depressed about the coxa. This exposes the pointed, posteriorly directed protrusions from each coxa. (D) The right coxal protrusion covered by overlapping microtrichia. (E) The microtrichia at still higher magnification.

The Journal of Experimental Biology

The Journal of Experimental Biology (2014) doi:10.1242/jeb.105429

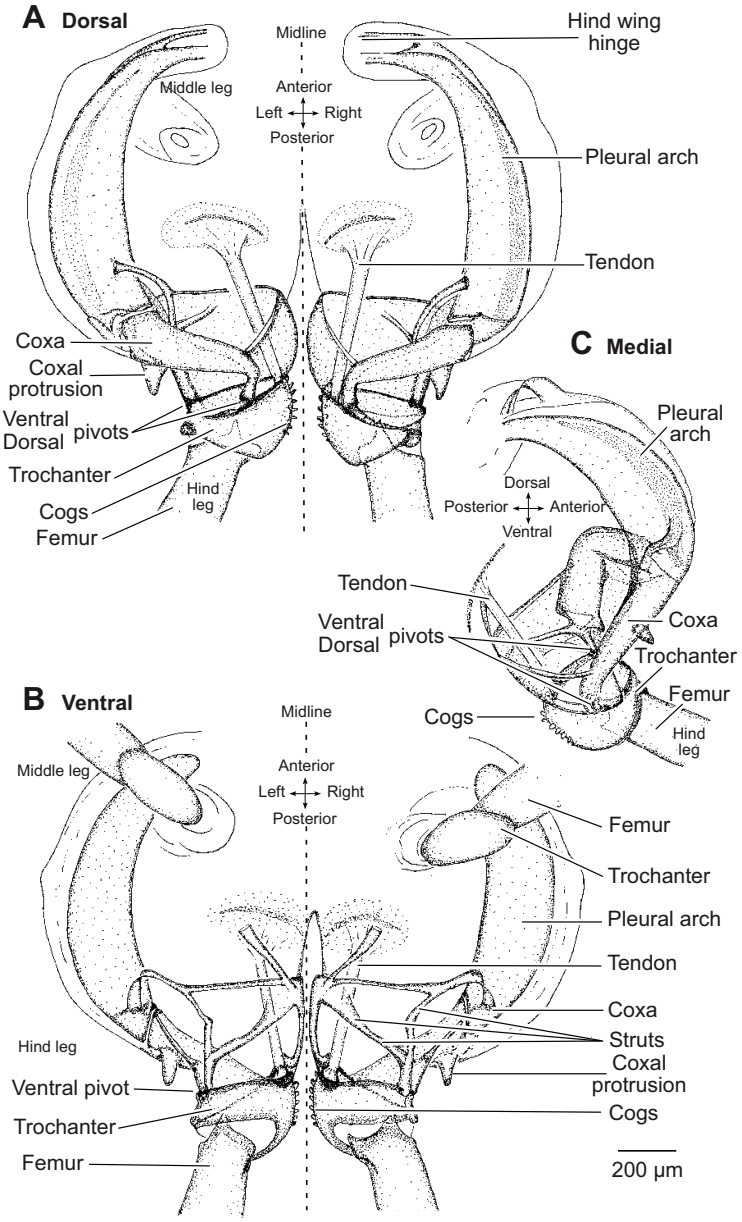

Fig. 4. Drawings of the skeletal supports for the proximal joints of the hind legs in a nymphal *M. pruinosa*. The internal soft tissues were dissolved in potassium hydroxide. (A) Dorsal view of the thorax revealing the large tendons of the trochanteral depressor muscles and the pleural arches linking each coxa to a wing hinge. (B) Ventral view showing the framework of cuticular supports and struts reinforcing the coxae. (C) The right pleural arch viewed medially to show the ventral and dorsal articulations of the trochantera with the coxae. Cogs are present on the medial surface of each hind trochanter

hind legs were fully levated in preparation for a jump, the left and right protrusions each contacted a raised, flat and smooth area on a dorsal hind femur (see inset in Fig. 2B). Patches of hairs that were longer and thicker than those elsewhere on the femur were present on the proximal and distal edges of this patch, located so as to suggest a possible proprioceptive role. The walls of the coxae were stiffened by a series of struts that were made visible by rendering the opaque cuticle transparent by treatment with potassium hydroxide (Fig. 4A–C). These struts ran from the medial and lateral pivots to the anterior rim of the coxa and to the lateral junction of the coxa with the pleural arches. Again, the defining feature appears to be to provide stable structures that can support the application of the high forces needed to generate a jump. A strip of cogs was present on the medial surface of each trochanter in nymphs (Fig. 4A–C) but were not present in adults (Fig. 2B, Fig. 3A), as in other planthopper species (Burrows and Sutton, 2013; Heilig and Sander, 1986).

The paired metathoracic pleural arches were also large structures relative to those in the meso- and prothorax. An arch curved anteriorly and dorsally from the ventral and lateral edge of the coxa to the articulation of the hind wing (Figs 4, 5). When illuminated with UV light (see Materials and methods for details of wavelengths) and viewed either ventrally (Fig. 5A) or from a side view looking laterally from the midline (Fig. 5B), an arch fluoresced bright blue. The intensity of this fluorescence was sensitive to the pH of the bathing saline; when the pH was made acidic it decreased but recovered when the pH was returned to 7.0 and then became more intense in more alkaline pH.

Muscles and tendons

The metathorax was dominated by a pair of bilaterally symmetrical trochanteral depressor muscles that together comprised ~10% of body mass. Each muscle consisted of many long parallel fibres (Burrows et al., 2014) that arose from an anterior phragma made of tergal and pleural plates. These fibres then inserted onto an umbrella-shaped apodeme (tendon), which then abruptly narrowed and ran through the coxa to insert onto the medial part of the trochanter (Fig. 2B, Fig. 4A,B). The paired trochanteral levator

The Journal of Experimental Biology (2014) doi:10.1242/jeb.105429

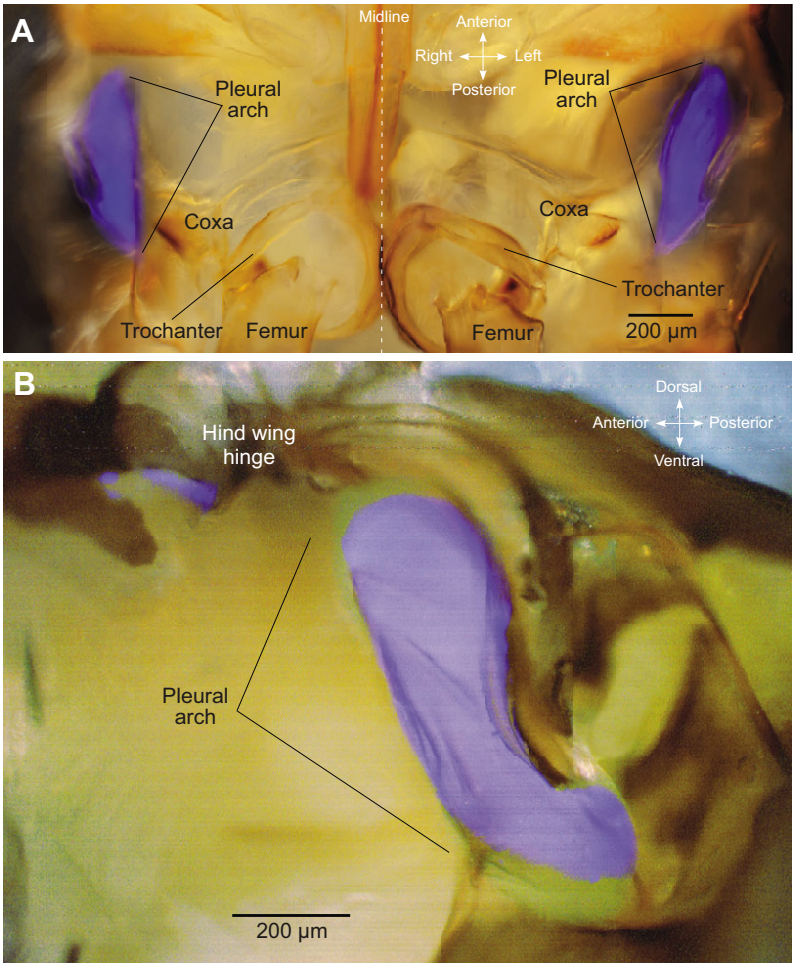

Fig. 5. Energy storage mechanisms and the presence of resilin. (A) Ventral view (as in Fig. 2B) of the thorax of an adult *M. pruinosa* after removal of the membranous ventral cuticle and underlying muscles. Images illuminated with white and then UV light have been superimposed to show that the pleural arches on both sides of the body fluoresce bright blue. (B) Side view of the thorax of an adult *C. peracutum* (oriented as in Fig. 4C) after a midline longitudinal section shows that the pleural arch fluoresces bright blue when illuminated with UV light. Some blue fluorescence is also present at the articulation of the hind wing with the thorax.

muscles were also located in the metathorax but were much smaller than the depressors.

Kinematics of the jump

In jumps by intact flatids viewed from the side, the wings obscured many of the crucial movements of the legs (Fig. 6; see supplementary material Movies 1, 2). What can be seen in these intact flatids is that the hind legs were largely responsible for providing the propulsive forces, particularly during the latter stages of a jump when the front and middle legs progressively lost contact with the ground before take-off. To reveal the sequence of leg movements and the angular changes of particular segments of a hind leg, the right wings were removed close to their articulation with the thorax (Fig. 7; see supplementary material Movie 3). This operation did not have a measurable effect on overall jump performance, as indicated either by the acceleration time (the time from the first detectable movement of a hind leg to the time when the insect became airborne) or by the velocity of the insect at take-off. Images of the jumping movements were also captured from below, as the insect jumped from a vertical glass wall of the chamber (Fig. 8; see supplementary material Movie 4), and from behind or in front, as the insect jumped away from and towards the camera, respectively. The figures specifically illustrate the jumps of *C. peracutum*, but a comparable analysis of the other two species showed the same sequence of events during jumping. The following description is therefore based on a compilation of all these different observations and analyses on all three species.

In preparation for a jump, both hind legs were first rotated forwards by levation of their trochantera about the stable coxae. The tibiae were also flexed about the femora. In this most forward levated position, the hind legs remained stationary for periods ranging from a few hundred milliseconds to seconds. The first detectable, propulsive movement of the hind legs was then a depression of the trochantera (Figs 7, 8). The trochantera of the two hind legs moved within one frame or 0.2 ms of each other. This was the minimum time resolution possible with a frame rate of 5000 s^{-1}. In other planthoppers where jumps have been captured at six times this frame rate, the synchronisation was within 0.03 ms (Burrows, 2009; Burrows and Bräunig, 2010).

As the depression of a trochanter continued, most easily seen by the changing angle of the femur relative to the body, the tibia was also extended about the femur, and the whole ventral surface of the tarsus was pushed against the ground. The consequence of these movements was that the body was progressively raised and in turn this lifted the front and middle legs from the ground. The hind legs were the only legs in contact with the ground during the last stages of the jump. The front legs showed no changes in their joint angles that could be related to any propulsive actions. Similarly, the middle legs showed only small depression movements of the trochanter and extension movements of the tibia.

During the acceleration phase of a jump, the angle of the body relative to the ground remained stable and did not rotate in the pitch roll, or yaw planes (Figs 6, 7). At take-off, the head of *C. peracutum* and *S. acuta* pointed downwards at an angle that varied between −16

The Journal of Experimental Biology (2014) doi:10.1242/jeb.105429

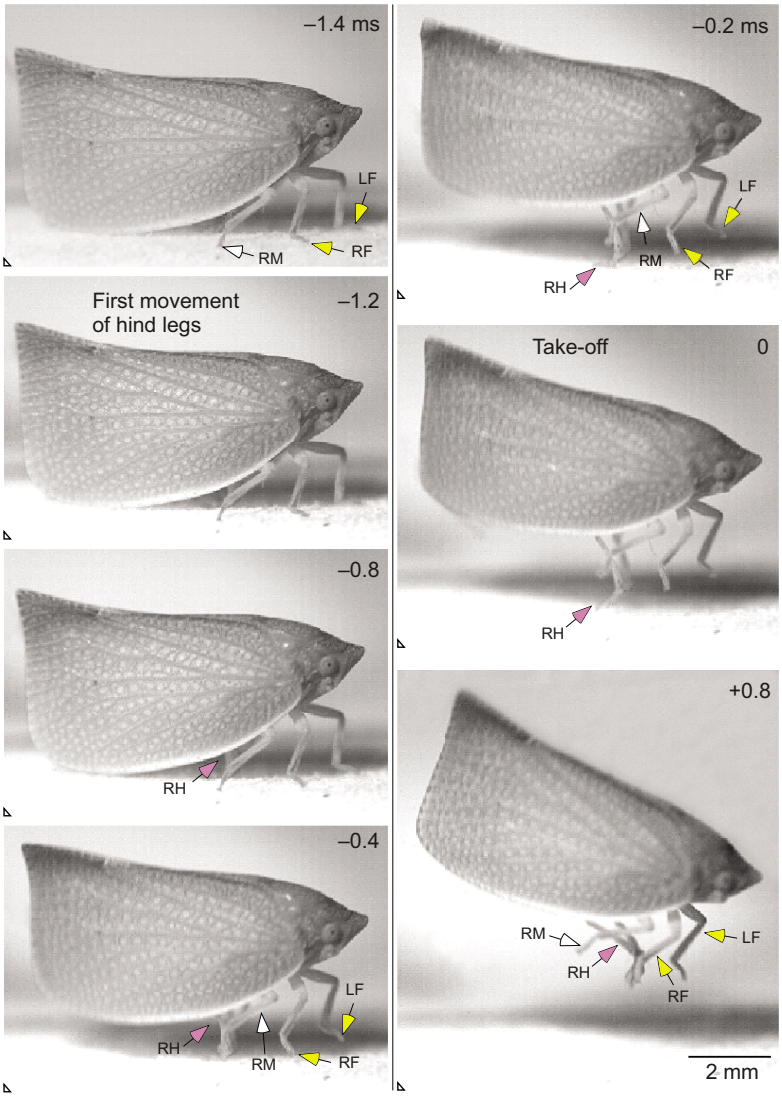

Fig. 6. Side view of a jump by *S. acuta* from a horizontal surface. Images were captured at a rate of 5000 images s^{-1} and with an exposure time of 0.05 ms. In this and subsequent figures these conventions are followed: selected images are arranged in two columns at the times indicated, with take-off designated as *t*=0 ms; the triangle at the bottom left-hand corner of each image represents a constant point of reference. The front (F) legs are indicated by arrows with yellow heads, the middle (M) legs by arrows with white heads and the hind (H) legs by arrows with pink heads. L and R denote left and right, respectively.

and −24 deg relative to the horizontal (Table 2). In *M. pruinosa*, the head was closer to being parallel with a mean angle of 4 deg. The downwards pitch of the head was not sufficient to lead to the body spinning. In contrast to the angles of the body, the angles of the trajectories were steep, with a range from 50 to 90 deg. All observations indicated that the body remained stable in all three planes at take-off.

Plotting the changing positions of particular points on the body and on a hind, middle and front leg showed the progressive movements in detail (Fig. 9). The tarsi of the front and middle legs followed the movements of the centre of mass, located on the body just behind the hind legs. By contrast, the hind tarsus remained on the ground, providing the thrust. Movements of the hind trochanter and tibiae began at the same time and their angular changes progressed together. The velocity of the movement increased progressively, peaking ~0.4 ms before take-off and then declining as the hind tarsi peeled off the ground with the terminal segments the last to lose contact. In intact insects, the wings did not open during the acceleration phase of the jump or even during the initial few milliseconds when airborne. The wings therefore made no propulsive contribution to a jump and only later did they contribute to forwards locomotion through flight.

Nymphs of *M. pruinosa* jumped readily like the adults with which they lived freely in groups. The kinematics of jumping were the same as in adults, although the hind legs were proportionately longer than the other legs compared with adults, and the movements of the hind trochantera were synchronised by interacting sets of gears. In contrast to adults, the body subtended a larger angle relative to the horizontal so that the head pointed upwards. The trajectory of the jump was also more variable with values ranging from 30 to 100 deg when they were moving backwards.

Jumping performance

The preceding measurements of the kinematics of a jump enable calculations of performance to be made (Table 2). The mean acceleration times for both adults and nymphs ranged only between 1.6 and 1.8 ms, with the fastest acceleration of 1.4 ms recorded in one *S. acuta*. Mean take-off velocities ranged from 1.8 to 2.3 m s^{-1} in the different species, with the highest velocity of 3.2 m s^{-1} recorded in one *C. peracutum*. These high velocities coupled with short acceleration times resulted in values of mean accelerations in adults of 1110 to 1350 m s^{-2}, with the highest individual values reaching 1960 m s^{-2} in *S. acuta*. This means that all adults and nymphs experienced forces of between 100 and 200 ***g***. The energy required to generate these jumps ranged from 107 μJ in the fastest jumps by the heaviest insects to 7 μJ, again in the fastest jumps by the lighter nymphs. On the basis that both trochanteral depressor

The Journal of Experimental Biology (2014) doi:10.1242/jeb.105429

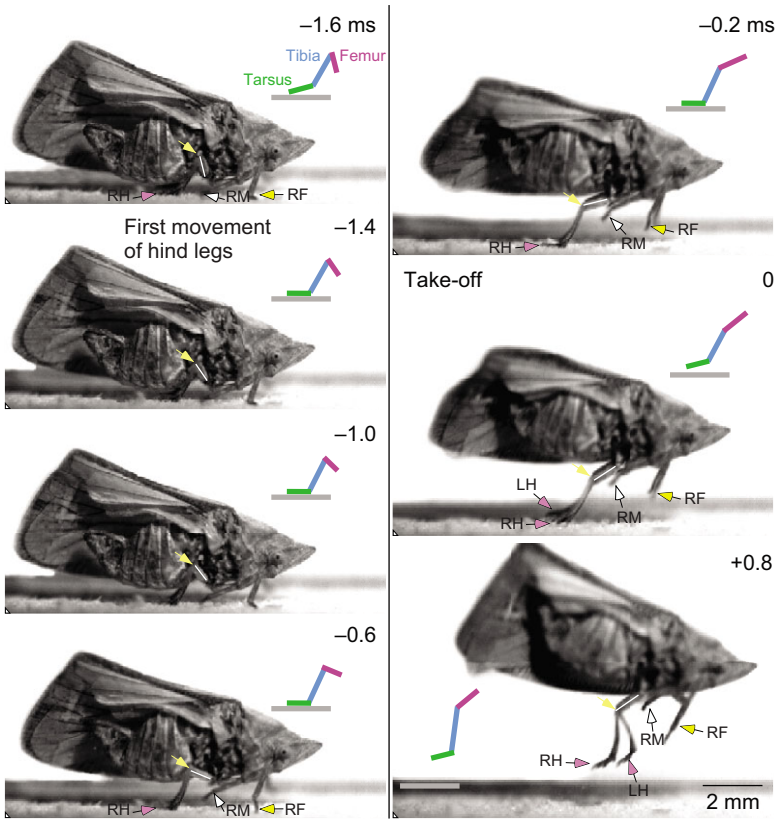

Fig. 7. Side view of a jump by *C. peracutum* from a horizontal surface. The right front wing was removed to enable movements of the joints of the right hind leg to be seen. The changing positions of the femoro-tibial joint of the right hind leg are indicated by diagonal pale yellow arrows and of the right hind femur with white lines. The images were captured at rate of 5000 images s^{-1} and with an exposure time of 0.05 ms. The stick diagrams show the positions of the femur (pink), tibia (cyan) and tarsus (green) of the right hind leg in the corresponding frame. The horizontal grey bar indicates the ground. See Fig. 6 for an explanation of the conventions used.

muscles comprised ~10% of body mass, as also found in other planthoppers (Burrows and Bräunig, 2010), both adults and nymphs needed a power output of 14,799 to 29,160 W kg^{-1} of muscle in their fastest jumps.

To estimate the distance (s) and height (h) reached in a jump, calculations were made according to Eqns 1 and 2 below that describe the motion of an inert body (Alexander, 1968):

$$s = v\cos\Theta\,(2v\sin\Theta / 9.81), \quad (1)$$

$$h = (v\sin\Theta)^2 / (2 \times 9.81), \quad (2)$$

where v is the velocity at take-off and Θ is the take-off angle. On this basis, adult *C. peracutum* and *M. pruinosa* are predicted to jump from a horizontal surface a distance of 950 mm and 840 mm, respectively, and to reach heights of 370 mm and 250 mm. These jumps represent a distance of more than 100 body lengths. By contrast, *S. acuta*, because of its steeper trajectory, would jump a distance of only 180 mm (equivalent to 20 body lengths) but reach a greater height of 400 mm. Nymphs of *M. pruinosa* would jump a distance of 340 mm (almost 100 body lengths) and reach a height of 210 mm. The effect of wind resistance is not considered in these estimates.

Landing

The high velocity of take-off propelled by jumping suggests that landing again might require wing movements to add stability and reduce velocity while the legs assume a posture that would contact with the ground over a broad and stable base. Far fewer landings than take-offs were captured because landing sites were unpredictable. Those apparently controlled landings that were captured all had the same pattern of leg movements (Fig. 10). As a landing site was approached, the front legs were spread forwards and laterally in the same plane as the under surface of the body and with the tibiae extended about the femora. The middle legs were extended downwards so that the tibiae were level with the lateral edges of the body. The hind legs also pointed downwards, but their tarsi were closer together under the midline of the body. Some 10–12 ms before touch down, the wings were in the depression phase of the wing beat cycle, but at the point of touch down they were being elevated. The hind tarsi touched down first, followed by the middle tarsi and finally the front tarsi. Such a sequence led to a controlled and stable touch down in which flexion of the femoro-tibial joints and levation of the coxo-trochanteral joint acted as shock absorbers. The wings were then folded, and walking was then able to take place.

DISCUSSION

This paper has shown that in their best jumps, adults of three species of flatids accelerated rapidly in 1.4 to 1.8 ms to take-off velocities of 2.8–3.2 m s^{-1} so that they experienced forces as high as 200 ***g***. They were propelled largely by rapid depression of the hind legs, which were 30% longer than the other legs but were only half or less the length of the body. The length of the hind legs does not, however, affect the take-off velocity when a catapult mechanism is used, because the release of energy stored in elastic cuticular structures is nearly independent of strain rate (Alexander, 1995; Bennet-Clark, 1990). No jumps were accompanied by movements of the large, triangular-shaped wings that extended above and behind the body and gave a laterally compressed appearance. The wingless nymphs of one species, which lived in groups together with the adults, were also adept jumpers but reached lower velocities at take-off than the adults. The wax that they secrete from the abdomen, often forming tufts that project posteriorly, can prevent ensnarement in spider webs and drowning if inadvertently landing on water (Eisner et al., 2005).

The Journal of Experimental Biology (2014) doi:10.1242/jeb.105429

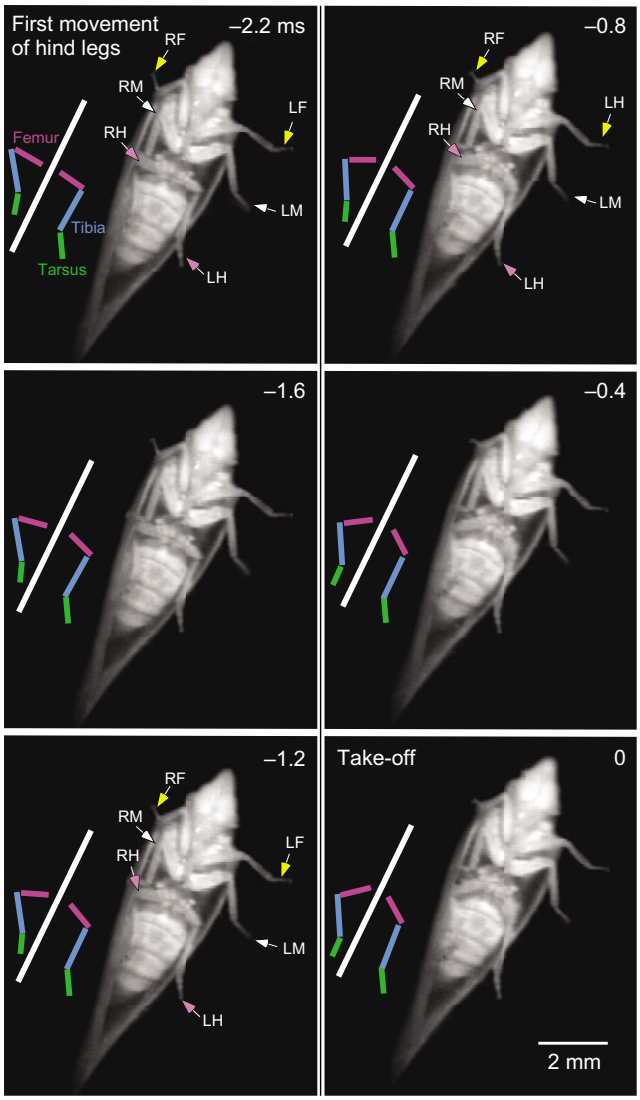

Fig. 8. Jump by *C. peracutum* viewed from underneath. Take-off at *t*=0 ms was from the horizontal glass floor of the chamber. Images were captured at a rate of 5000 images s^{-1} and with an exposure time of 0.05 ms. The stick diagrams show the midline longitudinal axis of the body (white) and the positions of the femur (pink), tibia (cyan) and tarsus (green) of the left and right hind legs, at the times indicated. See Fig. 6 for an explanation of the conventions used.

Power output and energy storage for jumping

Calculations from the kinematics indicate that the power requirements for the best jumps ranged from 25,000 to 29,000 W kg^{-1} in all three species analysed. By contrast, direct contraction of muscle can only produce power outputs of 250–500 W kg^{-1} (Askew and Marsh, 2002; Ellington, 1985; Josephson, 1993; Weis-Fogh and Alexander, 1977). Jumping in flatids, as in other hemipteran planthoppers (Burrows, 2009), froghoppers (Burrows, 2007c), leafhoppers (Burrows, 2007a) and treehoppers (Burrows, 2013), must therefore also involve power amplification. A catapult mechanism is used by fleas (Bennet-Clark and Lucey, 1967), locusts (Bennet-Clark, 1975) and hemipteran bugs to achieve this amplification. Recordings from the jumping muscles (extensor tibiae) of locusts (Burrows and Morris, 2001) and from trochanteral depressor muscles of froghoppers (Burrows, 2007c), leafhoppers (Burrows, 2007a) and from a species in the

Table 2. Jumping performance of flatids

	Body mass (*m*)	Acceleration time (*t*)	Take-off velocity (*v*)	Take-off angle (Θ)	Body angle at take-off	Acceleration	*g* force	Energy (*E*)	Power (*P*)	Force (**F**)	Power/kg muscle
Formula						*f*=*v*/*t*	***g***=*f*/9.81	*E*=0.5*m* v^2	*P*=*E*/*t*	**F**=*mf*	*p*/(0.1*m*)
Units	mg	ms	m s^{-1}	deg	deg	m s^{-2}	***g***	µJ	mW	mN	W kg^{-1}
C. peracutum											
Mean (*N*=8)	19.3±1.3 (*N*=29)	1.7±0.9	1.9±0.1	62.6±3.4	−16.2±4.4	1140	115	36	21	22	11,100
Best	20.4	1.8	3.2	57	5	1800	184	107	60	37	29,160
S. acuta											
Mean (*N*=3)	13.7	1.6	1.8	90	−24	1110	110	22	14	16	9730
Best	14.2	1.4	2.8			1960	200	53	38	28	27,000
M. pruinosa, adults											
Mean (*N*=3)	8.3±0.9 (*N*=7)	1.7	2.3	53	4	1350	138	14	8	7	15,560
Best	9.6	1.7	2.9	50	−10	1710	174	22	13	9	24,735
M. pruinosa, nymphs											
Mean (*N*=3)	2.9±0.3 (*N*=3)	1.7	1.8	33	58	1060	108	5	3	3	9570
Best	2.6	1.7	2.2	100	68	1295	132	7	4	3	14,230

The jumping performance of the three species of flatid analysed. Data in the five columns on the left are the mean of means + s.e.m. for the performance of (*N*) individuals of each species; the best performance (defined by take-off velocity) of a particular individual is also given. The calculated values in the five columns on the right are derived from these measured data.

The Journal of Experimental Biology (2014) doi:10.1242/jeb.105429

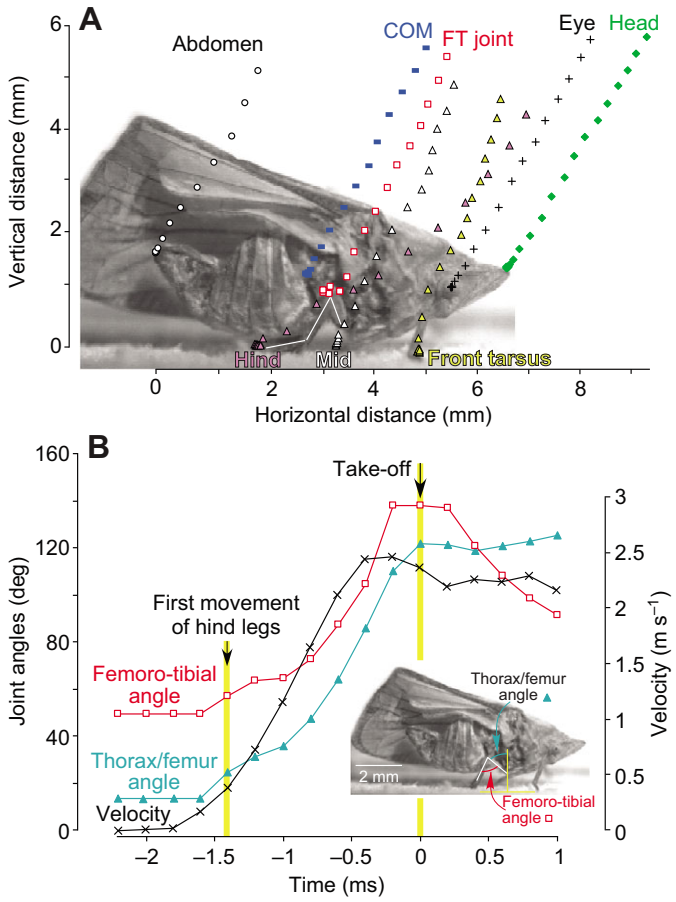

Fig. 9. Body positions and angular changes at hind leg joints during a jump. (A) The displacement of parts of the body [abdomen, centre of mass (COM)], eye and tip of head, the tarsi of the three right legs (triangles) and the hind femoro-tibial joint (FT joint; red open squares) are plotted for the jump in Fig. 7. The positions of each of these points at the start of a jump are superimposed onto a photograph of *C. peracutum* that was captured at the same time. (B) Changes in the angle between the thorax and the hind femur (blue triangles), the femoro-tibial angle (open red squares) (angles are indicated on the inset photograph) and the velocity of the flatid (plotted as a rolling three-point average; this results in the acceleration appearing to be applied before the legs started to move). The yellow vertical bars show the time when the hind legs first moved and the time of take-off (0 ms).

family Issidae (planthoppers) (Burrows and Bräunig, 2010) show that the muscles contract for a long time before the beginning of the propulsive movements of the hind legs. In hemipteran bugs, the muscle contractions during this preparatory stage of a jump, distort and bend part of the internal skeleton of the metathorax (the pleural arches) that link coxae to the hinges of the hind wings. Energy from the slow muscle contractions is thereby stored gradually and then released suddenly to power the rapid movements of the hind legs.

In froghoppers, the pleural arches are bow-shaped and are built of a composite of hard cuticle and the rubber-like protein resilin (Burrows et al., 2008). In the flatids analysed here, the pleural arches of the hind legs were observed to bend in preparation for a jump and then to unfurl as the hind legs rapidly extended. They therefore act like the pleural arches in froghoppers and issid and dictyopharid planthoppers (Burrows, 2009; Burrows, 2014; Burrows et al., 2008). In flatid planthoppers, these structures also fluoresced bright blue under illumination by specific wavelengths of UV light. The properties of this fluorescence were the same as those emitted by the pleural arches of froghoppers, which has been analysed in detail (Burrows et al., 2008). Two key signatures of resilin are met by the specificity of the emissions and by their dependence on the pH of a bathing solution (Neff et al., 2000). Furthermore, in the planthopper *Delphacodes* sp. (Hemiptera, family Delphacidae) and in froghoppers (Hemiptera, family Cercopidae), the fluorescence in the pleural arches precisely matches (Burrows et al., 2011) the staining with an antibody raised against gene CG15920 in *Drosophila melanogaster* (Elvin et al., 2005). The first exon of this gene expresses a soluble protein that, when cross-linked, forms a resilient, rubbery hydrogel called Rec-1 resilin in *Escherichia coli*. The antibody also stains resilin in three other insect orders (Lyons et al., 2011). These three criteria indicate that the pleural arches contain resilin in both planthoppers and froghoppers. This is further evidence that resilin and hard cuticle form a composite material that can serve four functions: (1) store the requisite energy for a jump; (2) withstand bending strains without fracturing; (3) unfurl to deliver the stored energy to power a jump; (4) return the body to its original shape in readiness for another jump (Burrows et al., 2008).

Jumping performance

The heads of the flatids analysed either pointed downwards at take-off or, as in *M. pruinosa*, were parallel with the ground. The trajectories of a jump were, however, variable with a range from 50 deg, which is close to the optimum for achieving maximal distance, to 90 deg, which would give maximal height. From these measurements of trajectories and take-off velocities, a jump was estimated to propel a flatid from a horizontal surface as far as 950 mm, or more than 100 times its body length. The maximum height achieved was 400 mm in *S. acuta*, but it was at the expense of distance. Jumps in their natural habitat will be from the different angles subtended by the leaves or branches of plants, so that gravity will have different effects. Moreover, none of the calculations take into account the considerable drag that will be experienced (Bennet-Clark and Alder, 1979; Vogel, 2005). Vogel has estimated that the froghopper *Philaenus*, which has a mean mass of 12 mg and a mean length of 6.1 mm (Burrows, 2006) and is thus similar in size to the flatids here, would lose some 25% of its jumping range because of drag (Vogel, 2005). The flatids might therefore be expected to have their jumping distances and heights reduced by a similar amount. In contrast to froghoppers and many families of planthoppers, the body and legs are enclosed by large stiff front wings, which means that the body is flattened laterally and has a smooth profile. These features suggest streamlining but such an assumption needs to be tested by wind tunnel measurements. If correct, body shape could improve jump distance and thus increase the likelihood that jumping will be an effective high-speed escape mechanism from predators and, therefore, is probably subject to natural selection. A powerful jump will also delay the need for flapping flight, which is likely to be slower and more visible to the same predators. Another family of planthoppers, the dictyopharids, take a different approach to possible streamlining by having an elongated and tapered head (Burrows, 2014). Indeed, some dictyopharids can match the performance of some issids that have a squat and blunt body shape by reaching a take-off velocity of 5 to 5.8 m s^{-1} (Burrows, 2009; Burrows, 2014).

The estimates of jump distance and height also do not take into account any contribution from movements of the wings. Before take-off, the wings always remained closed so that they made no contribution to a jump. Wing movements also did not occur in the first 4 ms after take-off or within the first 10 mm of travel along the

The Journal of Experimental Biology (2014) doi:10.1242/jeb.105429

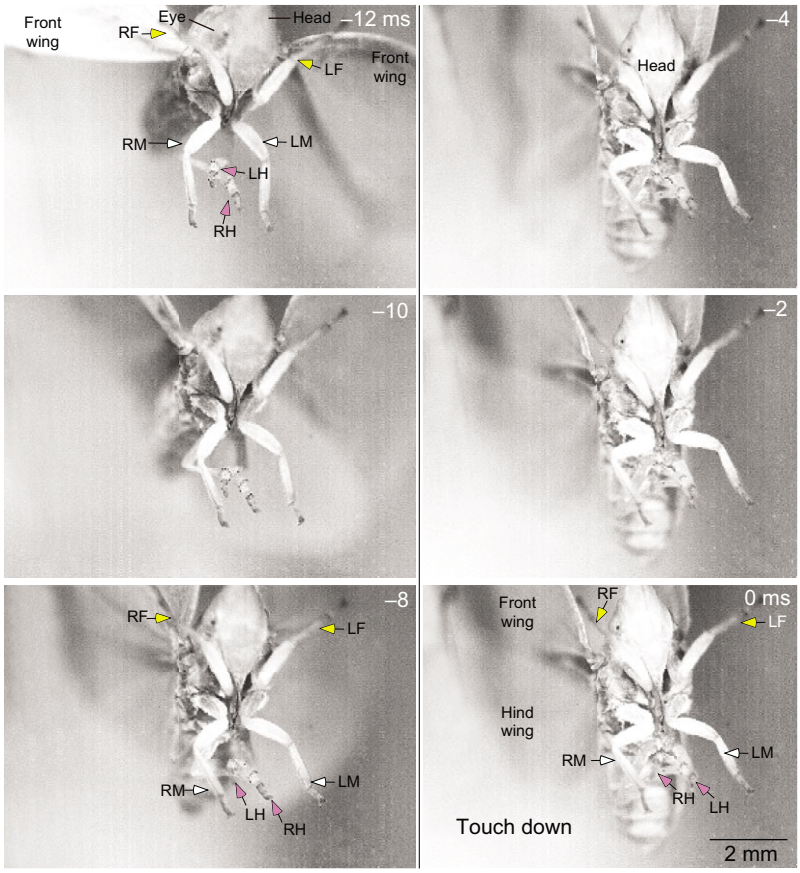

Fig. 10. Landing after a jump by *C. peracutum*. Images, at the times indicated, were captured at 5000 images s^{-1} and with an exposure time of 0.05 ms. In the approach to landing, the wings continued to flap and the front and middle legs were outstretched while the hind legs were flexed at their femoro-tibial joints. Touch down on the horizontal glass floor of the chamber occurred at time 0 ms. See Fig. 6 for an explanation of the conventions used.

jump trajectory. Opening of the wings does follow some jumps but the transition to flying was rarely captured. Some jumps do lead directly to flying and can also be inferred from images of landing when the wings were flapping. Just before touch down, the wings were depressed and all three pairs of legs were spread to provide a stable base. The hind legs touched down first by placement directly underneath the body.

Flatids therefore conform to the general principle of jumping in small insects. The power-producing muscles are located away from the segments of the legs that they propel. The mass of these segments is thus reduced, allowing them to be accelerated rapidly. The muscles contract slowly and have an ultrastructure that is characteristic of slowly contracting muscles (Burrows et al., 2014). The energy that they produce is stored over a prolonged period and then released suddenly so that the large power requirements of a jump can be met. This mechanism enables this fulgorid group of hemipterans with a wide range of body shapes to jump effectively.

Effects of body shape

An effect of body shape on jump performance emerges from a comparison of the three families of planthoppers so far analysed. *Issus coleoptratus* (family Issidae) pitches downwards or upwards at a mean rate of 43 Hz in the first few milliseconds after take-off, and before any wing movements are observed (Burrows, 2009). It also rotates at a slower rate in the roll plane. Dictyopharids are stable in the pitch and yaw planes but rotate at low rates in the roll plane (Burrows, 2014). Flatids showed no rotation in any plane. Instead, the winged adults lifted off with a steep trajectory with the body held stably as they climbed. The flatids thus generate the most stable jumps of the three families so far analysed. The large wings held along the sides of the body are the most obvious stabilising feature.

MATERIALS AND METHODS

Three species of flatid were analysed, which all belong to the order Hemiptera, suborder Auchenorrhyncha, superfamily Fulgoroidea, family Flatidae and sub-family Flatinae. Adult *C. peracutum* (the Australian citrus planthopper) and adult *S. acuta* (the Australian green planthopper) were collected on the campus of the University of Sydney, Sydney, NSW 2006, Australia, living individually on a variety of plants. Adults and nymphs of *M. pruinosa* were collected around Ljubljana, Slovenia, living in aggregations of many individuals and frequently covered with a white epicuticular wax (hence the species name *pruinosa*, meaning frosty). They are also known as the citrus planthopper, or the flatid planthopper, and are a recent (1979) introduction to Europe from North America (Zangheri and Donadini, 1980). The morphology of a fourth, unidentified species found in Danum, Sabah, Malaysia, was also studied.

The anatomy of the hind legs and metathorax was photographed and drawn in intact insects and in those preserved by fixation in 5% buffered formaldehyde and subsequent storage in 70% alcohol; fixation and storage in 70% alcohol or in 50% glycerol. To reveal details of the internal skeleton, the soft internal tissues and thin regions of the exoskeleton were removed by soaking in 10% potassium hydroxide for several days. Drawings of these structures were made with the aid of a drawing tube attached to a Leica MZ16 stereo microscope (Wetzlar, Germany). Colour photographs were taken with a Nikon DXM1200 digital camera attached to the same microscope. Fixed and dried specimens were mounted on holders, sputter coated with gold and then examined in a Philips XL-30 Scanning Electron Microscope (Philips, Eindhoven, The Netherlands). Lengths of the legs of fixed specimens were measured against a ruler to an accuracy of 0.1 mm on images captured with a digital camera attached to a Leica MZ16 microscope and projected onto a monitor. Body masses were determined to an accuracy of 0.1 mg with a Mettler Toledo AB104 balance (Beaumont Leys, Leicester, UK).

To search for the possible presence of the rubber-like protein resilin, flatids were viewed through Olympus MPlan ×5/0.1 NA and ×10/0.25 NA objective lenses, under UV or white epi-illumination on an Olympus

BX51WI compound microscope (Olympus UK, London). UV light from an X-cite series 120 metal halide light source (EXFO, Chandlers Ford, Hampshire, UK) was conditioned by a Semrock DAPI-5060B Brightline series UV filter set (Semrock, Rochester, NY, USA) with a sharp-edged (1% transmission limits) band from 350 to 407 nm. The resulting blue fluorescence emission was collected at wavelengths from 413 to 483 nm through a similarly sharp-edged bandpass filter and dichroic beam splitter.

Sequential images of jumps were captured at rates of 5000 s^{-1} and an exposure time of 0.05 ms for the two Australian species and at 4000 s^{-1} and an exposure time of 0.25 ms for *M. pruinosa* with a single Photron Fastcam 512PCI camera [Photron (Europe), West Wycombe, Buckinghamshire, UK). The images were fed directly to a computer for later analysis. Jumps occurred spontaneously, or were elicited by delicate mechanical stimulation with a fine silver wire or a paintbrush, in a chamber made of optical quality glass (width 80 mm, height 80 mm, depth 10 mm at floor level expanding to 25 mm at the ceiling). The floor was made of high density foam (Plastazote, Watkins and Doncaster, Cranbrook, Kent, UK). The camera, fitted with either a 100 mm micro Tokina lens or a 60 mm Micro Nikkor lens, pointed at the middle of this chamber. Measurements of distances moved and changes in joint angles were made from jumps that were parallel to the image plane of the camera, or as close as possible to this plane. Jumps that deviated from the image plane of the camera by more than 30 deg were not included in the analysis. Those that deviated by up to 30 deg were calculated to result in a maximum error of 10% in the measurements. Images were also captured from the underside of the body as a flatid jumped from a vertical (the front of the chamber) or horizontal (the floor of the chamber with the foam removed) glass surface. Selected image files were analysed with Motionscope camera software (Redlake Imaging, Tucson, AZ, USA) or with Canvas 14 (ACD Systems International, Seattle, WA, USA). Take-off was defined as the time at which the hind legs lost contact with the ground and the flatid became airborne, and was designated as t=0 ms, allowing different jumps to be compared. The acceleration time of a jump was defined as the period from the first detectable, propulsive movement of the hind legs until take-off. A one frame error in estimating both the first movement of the hind legs and the take-off time would result in a 10% error in measuring acceleration time. Peak velocity was calculated as the distance moved in a rolling three-point average of measurements taken from successive images, and the values presented are for the final milliseconds before take-off. Measurements are given as means ± s.e.m. Temperatures ranged from 25 to 30°C.

Acknowledgements

I am grateful to Steve Simpson and Meta Virant for the hospitality of their laboratories during my stays in Sydney, Australia and Ljubljana, Slovenia, respectively. I thank Steve Simpson, Swidi Ott and Steve Rogers for their help in collecting the Australian bugs and Murray Fletcher for identifying them. I also thank my Cambridge colleagues for their many helpful suggestions during the course of this work and for their comments on the manuscript.

Competing interests

The author declares no competing financial interests.

Funding

This research received no specific grant from any funding agency in the public, commercial or not-for-profit sectors.

Supplementary material

Supplementary material available online at
http://jeb.biologists.org/lookup/suppl/doi:10.1242/jeb.105429/-/DC1

References

Alexander, R. M. (1968). *Animal Mechanics*. London: Sidgwick and Jackson.
Alexander, R. M. (1995). Leg design and jumping technique for humans, other vertebrates and insects. *Philos. Trans. R. Soc. B* **347**, 235-248.
Askew, G. N. and Marsh, R. L. (2002). Muscle designed for maximum short-term power output: quail flight muscle. *J. Exp. Biol.* **205**, 2153-2160.
Bennet-Clark, H. C. (1975). The energetics of the jump of the locust *Schistocerca gregaria*. *J. Exp. Biol.* **63**, 53-83.
Bennet-Clark, H. C. (1990). Jumping in Orthoptera. In *Biology of Grasshoppers* (ed. R. F. Chapman and A. Joern), pp. 173-203. New York, NY: John Wiley and Sons.
Bennet-Clark, H. C. and Alder, G. M. (1979). The effect of air resistance on the jumping performance of insects. *J. Exp. Biol.* **82**, 105-121.
Bennet-Clark, H. C. and Lucey, E. C. A. (1967). The jump of the flea: a study of the energetics and a model of the mechanism. *J. Exp. Biol.* **47**, 59-67.
Burrows, M. (2006). Jumping performance of froghopper insects. *J. Exp. Biol.* **209**, 4607-4621.
Burrows, M. (2007a). Anatomy of the hind legs and actions of their muscles during jumping in leafhopper insects. *J. Exp. Biol.* **210**, 3590-3600.
Burrows, M. (2007b). Kinematics of jumping in leafhopper insects (Hemiptera, Auchenorrhyncha, Cicadellidae). *J. Exp. Biol.* **210**, 3579-3589.
Burrows, M. (2007c). Neural control and coordination of jumping in froghopper insects. *J. Neurophysiol.* **97**, 320-330.
Burrows, M. (2009). Jumping performance of planthoppers (Hemiptera, Issidae). *J. Exp. Biol.* **212**, 2844-2855.
Burrows, M. (2010). Energy storage and synchronisation of hind leg movements during jumping in planthopper insects (Hemiptera, Issidae). *J. Exp. Biol.* **213**, 469-478.
Burrows, M. (2013). Jumping mechanisms of treehopper insects (Hemiptera, Auchenorrhyncha, Membracidae). *J. Exp. Biol.* **216**, 788-799.
Burrows, M. (2014). Jumping mechanisms in dictyopharid planthoppers (Hemiptera, Dicytyopharidae). *J. Exp. Biol.* **217**, 402-413.
Burrows, M. and Bräunig, P. (2010). Actions of motor neurons and leg muscles in jumping by planthopper insects (Hemiptera, Issidae). *J. Comp. Neurol.* **518**, 1349-1369.
Burrows, M. and Morris, G. (2001). The kinematics and neural control of high-speed kicking movements in the locust. *J. Exp. Biol.* **204**, 3471-3481.
Burrows, M. and Sutton, G. (2013). Interacting gears synchronize propulsive leg movements in a jumping insect. *Science* **341**, 1254-1256.
Burrows, M., Shaw, S. R. and Sutton, G. P. (2008). Resilin and chitinous cuticle form a composite structure for energy storage in jumping by froghopper insects. *BMC Biol.* **6**, 41.
Burrows, M., Borycz, J. A., Shaw, S. R., Elvin, C. M. and Meinertzhagen, I. A. (2011). Antibody labelling of resilin in energy stores for jumping in plant sucking insects. *PLoS ONE* **6**, e28456.
Burrows, M., Meinertzhagen, I. A. and Bräunig, P. (2014). Slowly contracting muscles power the rapid jumping of planthopper insects (Hemiptera, Issidae). *Cell Tissue Res.* **355**, 213-222.
Cryan, J. R. and Urban, J. M. (2012). Higher-level phylogeny of the insect order Hemiptera: is Auchenorrhyncha really paraphyletic? *Syst. Entomol.* **37**, 7-21.
Eisner, T., Eisner, M. and Siegler, M. (2005). *Secret Weapons: Defenses of Insects, Spiders, Scorpions, and Other Many-Legged Creatures.* Cambridge, MA: The Belknap Press of Harvard University Press.
Ellington, C. P. (1985). Power and efficiency of insect flight muscle. *J. Exp. Biol.* **115**, 293-304.
Elvin, C. M., Carr, A. G., Huson, M. G., Maxwell, J. M., Pearson, R. D., Vuocolo, T., Liyou, N. E., Wong, D. C. C., Merritt, D. J. and Dixon, N. E. (2005). Synthesis and properties of crosslinked recombinant pro-resilin. *Nature* **437**, 999-1002.
Gorb, S. (2001). *Attachment Devices of Insect Cuticle*. Dordrecht; Boston, MA; London: Kluwer Academic Publishers.
Heilig, S. and Sander, K. (1986). Zahnradsektoren zur Koordination der Sprungbeine – eine lavale Synapomorphie der fulgoromorphen Zikaden (Homoptera, Cicadina, Fulgoroidea). *Zool. Jb. Syst.* **113**, 307-317.
Josephson, R. K. (1993). Contraction dynamics and power output of skeletal muscle. *Annu. Rev. Physiol.* **55**, 527-546.
Lyons, R. E., Wong, D. C. C., Kim, M., Lekieffre, N., Huson, M. G., Vuocolo, T., Merritt, D. J., Nairn, K. M., Dudek, D. M., Colgrave, M. L. et al. (2011). Molecular and functional characterisation of resilin across three insect orders. *Insect Biochem. Mol. Biol.* **41**, 881-890.
Neff, D., Frazier, S. F., Quimby, L., Wang, R.-T. and Zill, S. (2000). Identification of resilin in the leg of cockroach, *Periplaneta americana*: confirmation by a simple method using pH dependence of UV fluorescence. *Arthropod Struct. Dev.* **29**, 75-83.
Sander, K. (1957). Bau und Funktion des Sprungapparates von *Pyrilla perpusilla* WALKER (Homoptera – Fulgoridae). *Zool. Jb. Jena Anat.* **75**, 383-388.
Vogel, S. (2005). Living in a physical world II. The bio-ballistics of small projectiles. *J. Biosci.* **30**, 167-175.
Weis-Fogh, T. and Alexander, R. M. (1977). The sustained power output from striated muscle. In *Scale Effects in Animal Locomotion* (ed. T. J. Pedley), pp. 511-525. London: Academic Press.
Zangheri, S. and Donadini, P. (1980). Comparsa nel Veneto di un Omottero neartico *Metcalfa pruinosa* Say (Homoptera: Flatidae). *Redia (Firenze)* **63**, 301-305.

Movie 1. A jump by *Siphanta acuta* captured at 5000 frames s^{-1} and replayed at 10 frames s^{-1}. The insect is viewed from the side as it jumped from the floor of the experimental chamber. See also Fig. 6.

Movie 2. A jump by *Colgar peracutum* captured at 5000 frames s^{-1} and replayed at 10 frames s^{-1}. The insect is viewed from the side as it jumped from the floor of the experimental chamber.

Movie 3. A side view of a jump by *Colgar peracutum* captured at 5000 frames s^{-1} and replayed at 10 frames s^{-1} as it jumped from the floor of the experimental chamber. The right front wing was removed. See Fig. 7.

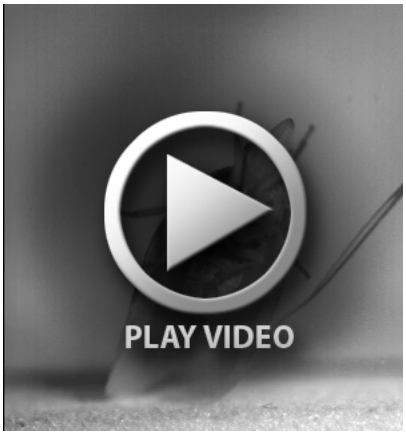

Movie 4. A ventral view of a jump by *Colgar peracutum* captured at 5000 frames s^{-1} and replayed at 10 frames s^{-1} as it jumped from the front glass wall of the experimental chamber. See also Fig. 8.